A Method for Forcing a Number of Motions or Rotations in 6 Degrees of Freedom Ship Simulators

Aurélien Babarit, Moran Charlou

Journal of Sailing Technology 20XX, volume X, issue X, pp. XX - XX.
The Society of Naval Architects and Marine Engineers.

A method for forcing a number of motions or rotations in 6 degrees of freedom ship simulators

Aurélien Babarit
Nantes Université, Centrale Nantes, CNRS, LHEEA, UMR6598, Fr. aurelien.babariut@ec-nantes.fr

Moran Charlou
Nantes Université, Centrale Nantes, CNRS, LHEEA, UMR6598, Fr.

Manuscript received [month] [day], [year]; revision received [month] [day], [year]; accepted [month] [day], [year].

Abstract. In this paper, a method is introduced which enables the forcing of any degrees of freedom in 6 DoFs ship simulator. It is based on the introduction of an extra force in the equation of motion of the ship and on the forcing of the second derivatives of the forced degrees of freedom rather than the forced degrees of freedom themselves. The method is explicit which makes it easy to implement in existing software. Examples of its application to oblique towing tests and forced heading in wind and waves are presented.

Keywords: ship simulator; forced degrees of freedom; performance prediction; Dynamic Velocity Prediction Program (DVPP); ship design

NOMENCLATURE

A	incident wave complex amplitude
$\mathbf{A}$	added mass matrix (6×6)
$\mathbf{A}_\infty$	added mass matrix at infinite frequency (6×6)
$\mathbf{B}$	radiation damping matrix (6×6)
$\mathbf{G}$	ship gravity centre [m]
$\mathbf{I_0}$	ship inertia matrix at center of gravity [kg.m^2]
k	incident wave number
$\mathbf{K}$	impulse response matrix (6×6)
$\mathbf{L_S}$	selection matrix (6×6)
m	ship mass [kg]
$\mathbf{M_T}$	total generalized mass matrix (6×6)
n	number of forced degrees of freedom
$\mathbf{O}$	origin of the North-East-Down (NED) reference frame [m]
$\mathbf{O}_b$	origin of the ship reference frame in NED reference frame [m]
p	x-component of the angular velocity in the ship reference frame [rad s^{-1}]
q	y-component of the angular velocity in the ship reference frame [rad s^{-1}]
q_r	r-component of the ship quaternion
q_i	i-component of the ship quaternion
q_j	j-component of the ship quaternion
q_k	k-component of the ship quaternion
r	z-component of the angular velocity in the ship reference frame [rad s^{-1}]
$\mathbf{R}_{NED,b}$	rotation matrix from ship reference frame to NED reference frame [-]
$\mathbf{T_{PG}}$	velocity transport operator from gravity centre to ship reference frame [-]
$\mathbf{T_{q\omega}}$	conversion operator of angular velocity to quaternion [-]
$\mathbf{T}_{\mathbf{\Xi}\lambda}$	conversion operator ($6 \times 6 - n$ matrix) of the $6 - n$ non-forced degrees of freedom λ to vector of non-
$\mathbf{T}_{\tau\mu}$	conversion operator ($6 \times n$ matrix) of the n components of the forcing extra force μ to the forcing extr
u	x-component of the ship velocity in the ship reference frame [m s^{-1}]
v	y-component of the ship velocity in the ship reference frame [m s^{-1}]
$\mathbf{v}_b$	velocity of the ship gravity centre [m s^{-1}]
$\mathbf{V}_u$	Generalized velocity vector [m s^{-1}, m s^{-1}, m s^{-1}, rad s^{-1}, rad s^{-1}, rad s^{-1}]
w	w-component of the ship velocity in the ship reference frame [m s^{-1}]
x	x-coordinate of the origin of the ship reference frame in the NED reference frame [m]
$\mathbf{x}_0$	x-axis of the North-East-Down reference frame [-]
$\mathbf{x}_b$	x-axis of the ship reference frame [-]
$\mathbf{X}_u$	Generalized position vector [m, m, m, rad, rad, rad]
y	y-coordinate of the origin of the ship reference frame in the NED reference frame [m]
$\mathbf{y}_0$	y-axis of the North-East-Down reference frame [-]
$\mathbf{y}_b$	y-axis of the ship reference frame [-]
z	z-coordinate of the origin of the ship reference frame in the NED reference frame [m]
$\mathbf{z}_0$	z-axis of the North-East-Down reference frame [-]
$\mathbf{z}_b$	z-axis of the ship reference frame [-]
β	true wind direction [°]
γ	wave propagation direction [°]
ξ_G	y-coordinate of the ship gravity centre in the ship reference frame [m]
$\mathbf{\Xi}$	vector of degrees of freedom [m, m, m, rad, rad, rad]
$\hat{\mathbf{\Xi}}$	vector of forced degrees of freedom [m, m, m, rad, rad, rad]
$\tilde{\mathbf{\Xi}}$	vector of non-forced degrees of freedom [m, m, m, rad, rad, rad]
θ	pitch motion [°]
λ	vector of $6 - n$ non-forced degrees of freedom
μ	vector of n degrees of freedom of the forcing extra force $\hat{\tau}$
ζ_G	z-coordinate of the ship gravity centre in the ship reference frame [m]

τ generalized force vector [N, N, N, N.m, N.m, N.m]
$\hat{\tau}$ forcing extra force [N, N, N, N.m, N.m, N.m]
τ_{rad} radiation force vector [N, N, N, N.m, N.m, N.m]
τ_{dif} diffraction force vector [N, N, N, N.m, N.m, N.m]
φ roll motion [°]
ψ yaw motion [°]
χ_G x-coordinate of the ship gravity centre in the ship reference frame [m]
ω incident wave frequency
ω_b angular velocity from the NED reference frame to the ship reference frame [rad s^{-1}]
ω_e encounter frequency

1 INTRODUCTION

Ship simulators have been developed to assess the performance of a ship in various weather conditions. For sailing yachts, steady-state ship simulators are called Velocity Prediction Programs (VPPs). They were originally developed in the 1970s in the context of the development of the Measurement Handicapping System Cairoli, 2000. According to Day et al., 2002, modern VPPs are reliable tools for predicting sailing yacht speed in steady-states conditions.

The need to optimize maneuvers led to the later development of Dynamic VPPs (DVPPs) Oliver et al., 1987. 6 degrees of freedom DVPPs were first introduced by Day et al., 2002 (first DVPPs used to neglect the effect of sinkage and trim). In that work, quasi-steady forces were modelled using the Delft Systematic Yacht Hull Series Gerritsma et al., 1993 while unsteady forces due to wave action were modelled using the nonlinear Froude-Krylov approach (radiation and diffraction forces are obtained from linear potential flow theory while Froude-Krylov and hydrostatic forces are obtained by integration of the pressure over the instantaneous wetted surface). The aerodynamic loads were modelled using the IMS method Poor, 1986. The forces from the appendages were modelled assuming they behave like isolated lifting surfaces. In Harris, 2005, quasi-steady forces were computed from a panel code while unsteady loads were obtained from strip theory. In Kostia and Kobus, 2004, a DVPP dedicated to match racing is presented. Aerodynamic interactions between the sails of the two competing boats are taken into account by modelling the wake of the sails with horseshoe vortices. The DVPP presented in Kerdraon et al., 2020 has been developed to deal with multihulls equipped with hydrofoils. The most significant differences of their DVPP in comparison to earlier DVPPs include (i) the use of a polynomial model for the quasi-steady forces whose coefficients are obtained from CFD simulations and (ii) the use of a Vortex Lattice Method (VLM) to model the appendages. That DVPP has recently been coupled to a structural solver (based on Timoshenko beams) to investigate flutter risk for the appendages of high performance sailing yachts Kerdraon et al., 2023.

Dynamic models have also been developed for commercial vessels. Until the renewed interest in the use of wind for propulsion of those vessels, the focus was mostly on the prediction of motion and loads in waves Kring et al., 1996Kim et al., 2011. The equipment of cargo vessels with wind propulsion systems making their performance also dependent on wind, performance prediction programs for cargo vessels have been modified such that their modelling capabilities are becoming similar to that of VPPs or DVPPs. Examples of such ship simulators are described in Tillig and Ringsberg, 2020, Kjellberg et al., 2023 and Charlou et al., 2022.

Modern ship simulators are usually based on the nonlinear 6 DoFs equation of motion presented in Fossen, 2011 (or an equivalent formulation). Be it a yacht or a commercial ship, a practical difficulty in such simulators is that of heading control. Indeed, the specification of a heading control system is a challenging task for the naval architect, as even a simple PID controller requires the tuning of coefficients to adapt them to the case study. Moreover, in the design process, one may be interested in replicating towing tank tests for which a number of degrees of freedom are either blocked (e.g. yaw)

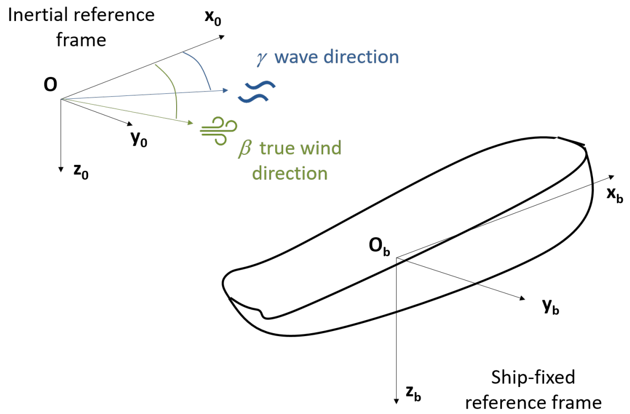

Figure 1. Basis reference frame and ship-fixed reference frame

or forced (e.g. horizontal ship position).

To these ends, a method that would allow forcing degrees of freedom is required. Such a method is not available in the literature to the authors' knowledge. The present paper addresses this gap. Moreover, another advantage of the proposed method is that it gives access to the force required for the forcing, which is useful information e.g for the design of the appendages or for the specification of the dynamometer in an oblique towing test.

The remainder of this paper is structured as follows. The proposed method is described in 2. Examples of its application to the simulation of an oblique towing test and to the simulation in wind and waves of a ship with forced heading are shown in section 3.1.

2 METHODS

2.1 Notations and conventions

The frames of reference are shown in Fig. 1. The North-East-Down (NED) reference frame is chosen as the inertial frame of reference ($\mathcal{R}_{\text{NED}}$). Its origin is $\mathbf{O}$. Its axis are $\mathbf{x}_0$ (pointing to the North), $\mathbf{y}_0$ (pointing to the East) and $\mathbf{z}_0$ (pointing down). The waves propagation direction is denoted γ. γ =0° corresponds to waves propagating to the North. The true wind direction is denoted β. β =0° corresponds to wind blowing to the North.

The frame of reference attached to the ship is $\mathcal{R}_b$. Its origin is $\mathbf{O}_b$. Its axis $(\mathbf{x}_b, \mathbf{y}_b, \mathbf{z}_b)$ are such as $\mathbf{x}_b$ points to the bow, $\mathbf{y}_b$ points to port and $\mathbf{z}_b$ points down.

The coordinates of the origin of the ship reference frame $\mathbf{O}_b$ in the inertial reference frame are denoted (x, y, z). Let $\mathbf{G}$ be the center of gravity of the ship. Its coordinates in the ship reference frame are denoted (χ_G, ξ_G, ζ_G). Its velocity relative to the inertial frame and expressed in the ship reference frame is denoted $\mathbf{v}^b = [u, v, w]^T$.

The ship rotations are denoted φ (roll), θ (pitch) and ψ (yaw). The ship reference frame is deduced from the NED reference frame using the usual Cardan/Tait-Bryan angles convention, i.e rotation of ψ about $\mathbf{z}_0$ first, then rotation of θ about the new y-axis, and finally rotation of φ about the new x-axis (equal to $\mathbf{x}_b$). The angular velocity from the NED reference frame to the ship reference frame is denoted $\omega^b = [p, q, r]^T$.

The ship mass is denoted m. Its inertia matrix at its center of gravity is denoted $\mathbf{I}_0$.

2.2 Equation of motion without forcing

Let us define $\mathbf{X}_u = [x, y, z, q_r, q_i, q_j, q_k]^T$ the generalized position vector, in which we recall that (x, y, z) are the coordinates of the ship reference frame origin, and in which $[q_r, q_i, q_j, q_k]$ is the quaternion corresponding to the rotation from the NED reference frame to the ship reference frame. For the Cardan/Tait-Bryan angles convention, there exist the simple following relationships between the ship rotations (roll, pitch, yaw angles) and the quaternion components Henderson, 1977:

- Pitch angle θ:

$$\sin\theta = 2(q_r q_j - q_i q_k) \tag{1}$$

- Roll angle φ:

$$\begin{aligned} \cos\varphi\cos\theta &= 1 - 2(q_i^2 + q_j^2) \\ \sin\varphi\cos\theta &= 2(q_r q_i + q_j q_k) \end{aligned} \tag{2}$$

- Yaw angle ψ:

$$\begin{aligned} \cos\psi\cos\theta &= 1 - 2(q_j^2 + q_k^2) \\ \sin\psi\cos\theta &= 2(q_i q_j + q_r q_k) \end{aligned} \tag{3}$$

Let $\mathbf{V}_u = [u, v, w, p, q, r,]^T$ be the generalized velocity vector. In the case where the degrees of freedom are not forced, the ship motion equation can be written as an ordinary differential equation of first order :

$$\begin{cases} \dot{\mathbf{X}}_u &= \mathbf{f}(\mathbf{X}_u, \mathbf{V}_u) \\ \dot{\mathbf{V}}_u &= \mathbf{M}_T^{-1}\{\sum_i \tau_{i,G}(t, \mathbf{X}_u, \mathbf{V}_u) + \mathbf{C}(\mathbf{V}_u)\mathbf{V}_u\} \end{cases} \tag{4}$$

Where:

- $\mathbf{f}$ is a function which relates the time derivative of the generalized position vector to the position vector and the generalized velocity vector. It can be written:

$$\mathbf{f} = \begin{cases} \mathbf{R}_{\text{NED},b}\mathbf{T}_{\mathbf{PG}}\mathbf{V}_u \\ \frac{1}{2}\mathbf{T}_{\mathbf{q}\omega}\omega_b \end{cases} \tag{5}$$

With:

$$\mathbf{T}_{\mathbf{q}\omega} = \begin{bmatrix} -q_i & -q_j & -q_k \\ q_r & -q_k & q_j \\ q_k & q_r & -q_i \\ -q_j & q_i & q_r \end{bmatrix} \tag{6}$$

And:

$$\mathbf{T_{PG}} = \begin{bmatrix} 1 & 0 & 0 & 0 & -\zeta_G & \xi_G \\ 0 & 1 & 0 & \zeta_G & 0 & -\chi_G \\ 0 & 0 & 1 & -\xi_G & \chi_G & 0 \end{bmatrix} \tag{7}$$

- $\mathbf{M_T}$ is the total generalized mass matrix. It is equal to the sum of the generalized mass matrix and the added mass matrix: $\mathbf{M_T} = \mathbf{M} + \mathbf{A}_\infty$. The generalized mass matrix reads: $\mathbf{M} = \begin{bmatrix} m\mathbf{I}_{3x3} & \mathbf{0}_{3x3} \\ \mathbf{0}_{3x3} & \mathbf{I}_0 \end{bmatrix}$
- $\tau_{i,\mathbf{G}}$ are the generalized external forces applying to the ship (gravity force, buoyancy force, wave-structure interaction force, hull resistance, appendages force, etc.). They are expressed at the ship COG $\mathbf{G}$ in the ship reference frame $\mathcal{R}_b$.
- $\mathbf{C}(\mathbf{V}_u)\mathbf{V}_u$ is the fictitious force. The operator $\mathbf{C}(\mathbf{V}_u)$ can be written:

$$\mathbf{C}(\mathbf{V}_u) = \begin{bmatrix} 0 & mr & -mq & 0 & 0 & 0 \\ -mr & 0 & mp & 0 & 0 & 0 \\ mq & -mp & 0 & 0 & 0 & 0 \\ 0 & 0 & 0 & 0 & -I_{zx}p - I_{zy}q - I_{zz}r & I_{yx}p + I_{yy}q + I_{yz}r \\ 0 & 0 & 0 & I_{zx}p + I_{zy}q + I_{zz}r & 0 & -I_{xy}q - I_{xz}r - I_{xx}p \\ 0 & 0 & 0 & -I_{yx}p - I_{yy}q - I_{yz}r & I_{xy}q + I_{xz}r + I_{xx}p & 0 \end{bmatrix} \tag{8}$$

Note that because of the off-diagonal terms of the generalized mass matrix M, the nonlinear terms in the equation of motion (fictitious force $\mathbf{C}(\mathbf{V}_u)$ and term $\mathbf{T_{q\omega}}\omega_b$ in 5) and the forces applying to the body, the degrees of freedom of the ship are coupled.

2.3 Equation of motion with forcing, extra force $\hat{\tau}$

Let us assume that an arbitrary number of degrees of freedom n among $\mathbf{\Xi} = [x, y, z, \varphi, \theta, \psi]^T$ are forced. Let $\hat{\mathbf{\Xi}}$ be the vector of the forced degrees of freedom such as to have its components $\hat{\Xi}_i$ equal to the forced motion if the degree of freedom i is forced ($1 \leq i \leq 6$), or equal to 0 otherwise. Let $\tilde{\mathbf{\Xi}}$ the vector of non-forced degrees of freedom complementary to $\hat{\mathbf{\Xi}}$, such as $\mathbf{\Xi} = \tilde{\mathbf{\Xi}} + \hat{\mathbf{\Xi}}$. That vector can be written:

$$\tilde{\mathbf{\Xi}} = \mathbf{T_{\Xi\lambda}}\lambda \tag{9}$$

where λ is the vector of the $6 - n$ non-forced degrees of freedom (thus $\mathbf{T_{\Xi\lambda}}$ is a $6 \times (6 - n)$ matrix).

The forcing is obtained by adding an extra force $\hat{\tau}$. Taking into account the extra force, the equation of motion becomes:

$$\begin{cases} \dot{\hat{\mathbf{X}}}_u = \mathbf{f}(\hat{\mathbf{X}}_u, \hat{\mathbf{V}}_u) \\ \dot{\hat{\mathbf{V}}}_u = \mathbf{M_T}^{-1}\{\sum_i \tau_{i,\mathbf{G}}(t, \hat{\mathbf{X}}_u, \hat{\mathbf{V}}_u) + \hat{\tau} + \mathbf{C}(\hat{\mathbf{V}}_u)\hat{\mathbf{V}}_u\} \end{cases} \tag{10}$$

where $\hat{\mathbf{X}}_u, \hat{\mathbf{V}}_u, \dot{\hat{\mathbf{V}}}_u$ are respectively the generalized position vector with forcing, the velocity vector with forcing and the acceleration vector with forcing (the forced degrees of freedom are taken into account in those vectors).

For the problem closure, the extra force must have n degrees of freedom. Therefore, without loss of generality, one can write the extra force as a function of n variables $\mu = \left[\mu_1, \ldots, \mu_n\right]$:

$$\hat{\tau} = \mathbf{T}_{\tau\mu}\mu \tag{11}$$

where $\mathbf{T}_{\tau\mu}$ is a $6 \times n$ matrix.

In theory, the operator $\mathbf{T}_{\tau\mu}$ can be chosen arbitrarily provided that it allows the forcing to be achieved (the corresponding mathematical condition is shown in section 2.5). However, in practice, one should be careful to select an operator $\mathbf{T}_{\tau\mu}$ representative to the case study. For example, in case one would like to model an oblique towing test in which both sinkage and trim are free, the z-components of the force and the moments must be 0. Therefore, all the elements of the third line and of the sixth line of $\mathbf{T}_{\tau\mu}$ must be equal to the zero in that case. In case of a forced heading, $\hat{\tau} = \mathbf{T}_{\tau\mu}\mu_1$ should represent the effect of the rudder. Thus, one may use $T_{\tau\mu} = \begin{bmatrix}0 & 1 & 0 & 0 & 0 & \chi_{rd}\end{bmatrix}^T$ with χ_{rd} be the x-coordinate of the rudder axis in the ship-fixed reference frame. By doing so, μ_1 is the side force delivered by the rudder.

With the forcing, the problem of determining the degrees of freedom which are forced is replaced by the problem of determining the extra force. This problem bears similarity with that of multibody systems modelling. Advanced methods have been developed to deal with such problems, including the articulated-body algorithm or the composite-rigid-body algorithm Featherstone, 2008, the Augmented formulation Negrut, 1998, the Discrete Euler-Lagrange equation Ham et al., 2015. Some have been applied to deal with problems relevant to the ocean engineering, such as lifting or lowering operations Cha et al., 2010; Ham et al., 2015; Wuillaume et al., 2021.

These methods are powerful but are also complex in their implementations, and for the user to specify the input data. Therefore, in the present study, a simpler method is proposed. The concept is to replace the forcing of the motion $\hat{\Xi}$ by the forcing of their second derivatives $\ddot{\hat{\Xi}}$, because (i) this will make the ship follow the prescribed forced motions provided that the initial conditions match that of the forced motion and (ii) it will be shown that it is relatively simple to relate the extra force to the second derivatives of the forced motion. Nevertheless, to make the method works, relationships between the second derivatives of the forced motion and the acceleration vector are required. They are developed in the following section.

2.4 Relationships between the forced motion and the acceleration vector

Let us consider first the case of pitch motion. By differentiating Eq. 1, one can show that the time derivatives of the pitch motion $\dot{\theta}$ and $\ddot{\theta}$ can be related to the time derivatives of the quaternion components:

$$\dot{\theta}\cos\theta = 2(\dot{q}_r q_j + q_r \dot{q}_j - \dot{q}_i q_k - q_i \dot{q}_k) \tag{12}$$

$$\ddot{\theta}\cos\theta - \dot{\theta}^2 \sin\theta = 2\mathbf{\Lambda}_\theta \ddot{\mathbf{Q}} + 4(\dot{q}_r \dot{q}_j - \dot{q}_i \dot{q}_k) \tag{13}$$

Where $\mathbf{\Lambda}_\theta = \begin{bmatrix} q_j & -q_k & q_r & -q_i \end{bmatrix}$ and $\ddot{\mathbf{Q}} = \begin{bmatrix} \ddot{q}_r & \ddot{q}_i & \ddot{q}_j & \ddot{q}_k \end{bmatrix}^T$.

Moreover, the time derivative of the angular velocity components $\dot{\omega}^b = \begin{bmatrix} \dot{p} & \dot{q} & \dot{r} \end{bmatrix}^T$ are related to the quaternion components according to:

$$\ddot{\mathbf{Q}} = \frac{1}{2}\mathbf{T}_{\mathbf{q}\omega}\dot{\omega}^b + \frac{1}{2}\dot{\mathbf{T}}_{\mathbf{q}\omega}\omega^b \tag{14}$$

Where $\dot{\mathbf{T}}_{\mathbf{q}\omega} = \begin{bmatrix} -\dot{q}_i & -\dot{q}_j & -\dot{q}_k \\ \dot{q}_r & -\dot{q}_k & \dot{q}_j \\ \dot{q}_k & \dot{q}_r & -\dot{q}_i \\ -\dot{q}_j & \dot{q}_i & \dot{q}_r \end{bmatrix}$

By combining Eq. 13 and Eq. 14, one can show:

$$\mathbf{\Lambda}_\theta \mathbf{T}_{\mathbf{q}\omega}\dot{\omega}^b = \ddot{\theta}\cos\theta + \sigma_\theta \tag{15}$$

Where:

$$\sigma_\theta = -\mathbf{\Lambda}_\theta \dot{\mathbf{T}}_{\mathbf{q}\omega}\omega^b - 4(\dot{q}_r\dot{q}_j - \dot{q}_i\dot{q}_k) - \dot{\theta}^2\sin\theta \tag{16}$$

Using the same procedure, relationships similar to Eq. 15 can be established for roll motion and yaw motion.

For roll motion, differentiation of Eq. 2 leads:

$$\ddot{\varphi}\cos\theta - 2\dot{\varphi}\tan\theta(\dot{q}_r q_j + q_r\dot{q}_j - \dot{q}_i q_k - q_i\dot{q}_k) = 2\mathbf{\Lambda}_\varphi\ddot{\mathbf{Q}} + 4(\dot{q}_r\dot{q}_i + \dot{q}_j\dot{q}_k)\cos\varphi - 2(\dot{q}_r q_i + q_r\dot{q}_i + \dot{q}_j q_k + q_j\dot{q}_k)\dot{\varphi}\sin\varphi \\ + 4(\dot{q}_i^2 + \dot{q}_j^2)\sin\varphi + 4(q_i\dot{q}_i + q_j\dot{q}_j)\dot{\varphi}\cos\varphi \tag{17}$$

Where:

$$\mathbf{\Lambda}_\varphi = \begin{bmatrix} q_i\cos\varphi & q_r\cos\varphi + 2q_i\sin\varphi & q_k\cos\varphi + 2q_j\sin\varphi & q_j\cos\varphi \end{bmatrix} \tag{18}$$

Combining Eq. 14 and Eq. 17 leads to:

$$\mathbf{\Lambda}_\varphi \mathbf{T}_{\mathbf{q}\omega}\dot{\omega}^b = \ddot{\varphi}\cos\theta + \sigma_\varphi \tag{19}$$

Where:

$$\sigma_\varphi = -\mathbf{\Lambda}_\varphi \dot{\mathbf{T}}_{\mathbf{q}\omega}\omega^b - 4(\dot{q}_r\dot{q}_i + \dot{q}_j\dot{q}_k)\cos\varphi + 2(\dot{q}_r q_i + q_r\dot{q}_i + \dot{q}_j q_k + q_j\dot{q}_k)\dot{\varphi}\sin\varphi \\ - 4(\dot{q}_i^2 + \dot{q}_j^2)\sin\varphi - 4(q_i\dot{q}_i + q_j\dot{q}_j)\dot{\varphi}\cos\varphi - 2\dot{\varphi}\tan\theta(\dot{q}_r q_j + q_r\dot{q}_j - \dot{q}_i q_k - q_i\dot{q}_k) \tag{20}$$

For yaw, differentiation of Eq. 3 leads:

$$\ddot{\psi}\cos\theta - 2\dot{\psi}\tan\theta(\dot{q}_r q_j + q_r\dot{q}_j - \dot{q}_i q_k - q_i\dot{q}_k) = 2\mathbf{\Lambda}_\psi\ddot{\mathbf{Q}} + 4(\dot{q}_i\dot{q}_j + \dot{q}_r\dot{q}_k)\cos\psi - 2(\dot{q}_i q_j + q_i\dot{q}_j + \dot{q}_r q_k + q_r\dot{q}_k)\dot{\psi}\sin\psi \\ + 4(\dot{q}_j^2 + \dot{q}_k^2)\sin\psi + 4(q_j\dot{q}_j + q_k\dot{q}_k)\dot{\psi}\cos\psi \quad (21)$$

Where:

$$\mathbf{\Lambda}_\psi = \begin{bmatrix} q_k\cos\psi & q_j\cos\psi & q_i\cos\psi + 2q_j\sin\psi & q_r\cos\psi + 2q_k\sin\psi \end{bmatrix} \quad (22)$$

Combining Eq. 14 and Eq. 21 leads to:

$$\mathbf{\Lambda}_\psi\mathbf{T}_{\mathbf{q}\omega}\dot{\omega}^b = \ddot{\psi}\cos\theta + \sigma_\psi \quad (23)$$

Where:

$$\sigma_\psi = -\mathbf{\Lambda}_\psi\dot{\mathbf{T}}_{\mathbf{q}\omega}\omega^b - 4(\dot{q}_i\dot{q}_j + \dot{q}_r\dot{q}_k)\cos\psi + 2(\dot{q}_i q_j + q_i\dot{q}_j + \dot{q}_r q_k + q_r\dot{q}_k)\dot{\psi}\sin\psi \\ - 4(\dot{q}_j^2 + \dot{q}_k^2)\sin\psi - 4(q_j\dot{q}_j + q_k\dot{q}_k)\dot{\psi}\cos\psi - 2\dot{\psi}\tan\theta(\dot{q}_r q_j + q_r\dot{q}_j - \dot{q}_i q_k - q_i\dot{q}_k) \quad (24)$$

Finally, by assembling Eqs. 15, 19, 23, one can write:

$$\mathbf{\Lambda}\dot{\mathbf{V}}_u = \cos\theta\begin{bmatrix}\ddot{\phi}\\ \ddot{\theta}\\ \ddot{\psi}\end{bmatrix} + \sigma \quad (25)$$

Where

- $\mathbf{\Lambda} = \begin{bmatrix} \mathbf{0}_{3x3} & \begin{bmatrix}\mathbf{\Lambda}_\phi\\ \mathbf{\Lambda}_\theta\\ \mathbf{\Lambda}_\psi\end{bmatrix}\mathbf{T}_{\mathbf{q}\omega} \end{bmatrix}$
- $\sigma = \begin{bmatrix}\sigma_\phi\\ \sigma_\theta\\ \sigma_\psi\end{bmatrix}$

By differentiating Eq. 5, one can show:

$$\begin{bmatrix}\ddot{x}\\ \ddot{y}\\ \ddot{z}\end{bmatrix} = \mathbf{R}_{\text{NED},b}\mathbf{T}_{\mathbf{PG}}\dot{\hat{\mathbf{V}}}_u + \dot{\mathbf{R}}_{\text{NED},b}\mathbf{T}_{\mathbf{PG}}\hat{\mathbf{V}}_u \quad (26)$$

Where $\dot{\mathbf{R}}_{\text{NED},b}$ is given in Appendix.

Finally, by assembling Eq. 25 and 26, one can write:

$$\ddot{\mathbf{\Xi}}\cos\theta = \mathbf{A_\Lambda}\dot{\hat{\mathbf{V}}}_u + \mathbf{B}_\sigma \tag{27}$$

Where:

- $\ddot{\mathbf{\Xi}} = \begin{bmatrix}\ddot{x} & \ddot{y} & \ddot{z} & \ddot{\phi} & \ddot{\theta} & \ddot{\psi}\end{bmatrix}^T$
- $\mathbf{A_\Lambda} = \begin{bmatrix}\mathbf{R}_{\text{NED},b}\mathbf{T_{PG}}\cos\theta \\ \mathbf{\Lambda}\end{bmatrix}$
- $\mathbf{B}_\sigma = \begin{bmatrix}\dot{\mathbf{R}}_{\text{NED},b}\mathbf{T_{PG}}\hat{\mathbf{V}}_u\cos\theta \\ -\sigma\end{bmatrix}$

Eq. 28 provides the required relationship between the second derivatives of the degrees of freedom and the acceleration vector.

2.5 Relationship between the extra force and the second derivatives of the forced degrees of freedom

Let us recall that by definition, the vector of degrees of freedom $\mathbf{\Xi}$ is equal to the sum of the vector of forced degrees of freedom $\hat{\mathbf{\Xi}}$ and the vector of the non-forced degrees of freedom $\tilde{\mathbf{\Xi}}$ ($\mathbf{\Xi} = \hat{\mathbf{\Xi}} + \tilde{\mathbf{\Xi}}$). Thus, using Eq. 10, the relationship between the second derivatives of the degrees of freedom and the acceleration vector (Eq. 28) can be rewritten such as to obtain a linear system relating the second derivatives of the non-forced degrees of freedom $\ddot{\tilde{\mathbf{\Xi}}}$ and the extra force $\hat{\tau}$ to the second derivatives of the forced degrees of freedom $\ddot{\hat{\mathbf{\Xi}}}$ and of the sum of the other forces :

$$\ddot{\hat{\mathbf{\Xi}}}\cos\theta + \ddot{\tilde{\mathbf{\Xi}}}\cos\theta = \mathbf{A_\Lambda}\mathbf{M_T}^{-1}\hat{\tau} + \mathbf{A_\Lambda}\mathbf{M_T}^{-1}\{\sum_i \tau_{i,\mathbf{G}}(t, \hat{\mathbf{X}}_u, \hat{\mathbf{V}}_u) + \mathbf{C}(\hat{\mathbf{V}}_u)\hat{\mathbf{V}}_u\} + \mathbf{B}_\sigma \tag{28}$$

By recognizing in this last equation the equation of motion without forcing (Eq. 4) and by rearranging the terms, one can show:

$$\mathbf{A}\mathbf{M_T}^{-1}\hat{\tau} - \ddot{\tilde{\mathbf{\Xi}}}\cos\theta = \ddot{\hat{\mathbf{\Xi}}}\cos\theta - \mathbf{A}\dot{\mathbf{V}}_u - \mathbf{B} \tag{29}$$

where $\dot{\mathbf{V}}_u$ is the acceleration vector without forcing as given by Eq. 4.

By definitions of the operators $\mathbf{T}_{\mathbf{\Xi}\lambda}$ and $\mathbf{T}_{\tau\mu}$ (Eqs. 9 and 11), Eq. 30 can be rewritten:

$$\mathbf{A}\mathbf{M_T}^{-1}\mathbf{T}_{\tau\mu}\mu - \mathbf{T}_{\mathbf{\Xi}\lambda}\cos\theta\ddot{\lambda} = \ddot{\hat{\mathbf{\Xi}}}\cos\theta - \mathbf{A}\dot{\mathbf{V}}_u - \mathbf{B} \tag{30}$$

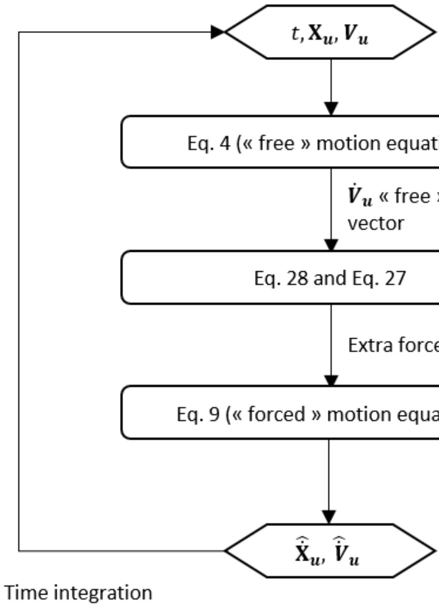

Figure 2. Procedure for the calculation of the extra force and of the forced acceleration vector

Therefore, let us define the vector $\mathbf{Y}$ assembling the second derivatives of the non-forced degrees of freedom and the components of the extra force: $\mathbf{Y} = \begin{bmatrix} \ddot{\lambda} \\ \mu \end{bmatrix}$. Eq. 30 can thus be rewritten:

$$\{\mathbf{A}\mathbf{M}_{\mathbf{T}}{}^{-1} \left[\mathbf{0}_{6\times 6-n} \quad \mathbf{T}_{\tau\mu}\right] - \cos\theta \left[\mathbf{T}_{\Xi\lambda} \quad \mathbf{0}_{6\times n}\right]\}\mathbf{Y} = \hat{\ddot{\Xi}} \cos\theta - \mathbf{A}\dot{\mathbf{V}}_u - \mathbf{B} \tag{31}$$

This last equation (combined with Eq. 11) can be used to determine the extra force - and thus the forced acceleration vector $\hat{\dot{V}}_u$ (using Eq. 10) - provided that the matrix $\{\mathbf{A}\mathbf{M}_{\mathbf{T}}{}^{-1} \left[\mathbf{0}_{6\times 6-n} \quad \mathbf{T}_{\tau\mu}\right] - \cos\theta \left[\mathbf{T}_{\Xi\lambda} \quad \mathbf{0}_{6\times n}\right]\}$ is invertible. This mathematical condition expresses whether the selected operator $\mathbf{T}_{\tau\mu}$ allows the desired forced movement to be achieved.

2.6 Procedure of calculation of the forced acceleration vector

In practice, the procedure is as follows. At the current time t, the generalized position vector $\mathbf{X}_u$ and generalized velocity vector $\mathbf{V}_u$ are known. Moreover, it is assumed that they are such that $\Xi = \hat{\Xi}$ and $\dot{\Xi} = \hat{\dot{\Xi}}$ (the forced degrees of freedom and their first derivatives have correctly been enforced up to the current time t). The first step is to compute the "free" acceleration vector $\dot{\mathbf{V}}_u$ using the "free" motion equation Eq. 4. The second step is then to calculate the extra force $\hat{\tau}$ using Eq. 31 and Eq. 11. The third step is to calculate the forced acceleration using Eq. 10 which is finally used by the time stepper to advance forward in time.

Figure 2 shows a graphical representation of the procedure.

3 Results

The method has been implemented in *xdyn*. *xdyn* is an open-source system-based method ship simulator which has mostly been developed by the company Sirehna *xdyn* n.d. It is a highly flexible simulation tool as it allows the user to define which forces to take into account among many options. To date, the available options include the hydrodynamics forces acting on the hull according to the MMG model Yasukama and Yoshimura, 2015, propeller(s) forces (including the Wageningen

	Full scale	1/110 scale
Hull		
L_{pp} (m)	320.0	2.902
B/L_{pp}	0.181	
d/L_{pp}	0.065	
∇/L_{pp}^3	0.00954	
C_b	0.81	
LCG/L_{pp}	0.035	
Propeller		
D_p/L_{pp}	0.0308	
Z	4	
P/D_p	0.721	
A_E/A_0	0.431	
Rudder		
A_r/L_{pp}^2	0.00133	
b/L_{pp}	0.0494	
Wind propulsion units		
Type	Soft sails	
Number	3	
A_s/L_{pp}^2	0.00977	
L_{s1}/L_{pp}	-0.3125	
L_{s2}/L_{pp}	0.	
L_{s2}/L_{pp}	0.3125	

Table 1. Main characteristics of the case study

B-series propellers Bernitsas et al., 1981), rudder forces, propeller and rudder forces taking into account interactions Blendermann et al., 1993, linear or nonlinear hydrostatic forces, wave forces (linear radiation forces, linear diffraction forces, linear or nonlinear Froude-Krylov forces), wind forces and wind propulsion units forces (through their aerodynamic coefficients). Moreover, controllers can be taken into account. *xdyn* has been validated for the case of the performance of an energy ship in calm water in Charlou et al., 2023. In its present state, *xdyn* can be used to simulate a single ship in open water with waves and wind. More complex situations such as a ship in confined waters or ships passing by each other would require further developments.

3.1 Case study

The case study is a KVLCC2 tanker *SIMMAN 2008 : Workshop Verification and Validation of Ship Manoeuvring Simulation Methods* n.d. equipped with three soft sails ($1000\,\mathrm{m}^2$ each) Charlou, 2023. Its main characteristics are shown in Table 1 at full scale and at 1/110 scale. It is of particular interest for this study because it includes wind propulsion, which introduces additional difficulty for course-keeping (because a course deviation results in a change of apparent wind angle which in turn changes the aerodynamic force from the sails).

The physical effects which are taken into account in the model are:

- Gravity force
- Hull resistance. It is modelled using the Holtrop & Mennen model Holtrop and Mennen, 1982.
- Maneuverability forces. They are modelled using the MMG model Yasukama and Yoshimura, 2015. The hydrodynamic derivatives are taken from that same source.
- Nonlinear hydrostatic and Froude-Krylov forces. In *xdyn*, they are obtained by integration of the hydrostatic pressure and the dynamic pressure due to the incident waves over the instanta-

neous wetted surface. Incident waves are modelled by superposition of elementary Airy waves. Stretching is applied for the prediction above the mean water level of physical quantities related to incident waves.

- Diffraction forces and radiation forces.
- Propeller and rudder forces. They are modelled according to Yasukama and Yoshimura, 2015.
- Sail forces. They are calculated from aerodynamic coefficients from the ORC VPP model (ORC), 2021.

In *xdyn*, diffraction forces and radiation forces are expressed according to linear potential theory. According to Bougis, 1980Horel, 2016, the radiation force $\tau_{rad,G}$ can be written:

$$\tau_{rad,G}(t, \mathbf{X_u}, \mathbf{V_u}, \dot{\mathbf{V}}_\mathbf{u}) = -\mathbf{A}_\infty \dot{\mathbf{V}}_\mathbf{u} + \mathbf{A}_\infty \mathbf{L_S}(\bar{\mathbf{V}}_\mathbf{u})(\mathbf{V_u} - \bar{\mathbf{V}}_\mathbf{u}) - \int_0^\infty \mathbf{K}(t', \bar{\mathbf{V}}_\mathbf{u}) \left(\mathbf{V_u}(t-t') - \bar{\mathbf{V}}_\mathbf{u}\right) dt' \quad (32)$$

Where $\mathbf{A}_\infty$ is the added mass matrix for infinite frequency and $\mathbf{K}(t', \bar{\mathbf{V}}_\mathbf{u})$ is the impulse response function taking into account the average horizontal velocities (forward speed and drift velocity) $\bar{\mathbf{V}}_\mathbf{u}) = \begin{bmatrix}\bar{u} & \bar{v} & 0 & 0 & 0 & 0\end{bmatrix}^T$; and where $\mathbf{L_S}(\bar{\mathbf{V}}_\mathbf{u})$ is the selection matrix:

$$\mathbf{L_S}(\bar{\mathbf{V}}_\mathbf{u}) = \begin{bmatrix} 0 & 0 & 0 & 0 & 0 & \bar{v} \\ 0 & 0 & 0 & 0 & 0 & -\bar{u} \\ 0 & 0 & 0 & -\bar{v} & \bar{u} & 0 \\ 0 & 0 & 0 & 0 & 0 & 0 \\ 0 & 0 & 0 & 0 & 0 & 0 \\ 0 & 0 & 0 & 0 & 0 & 0 \end{bmatrix} \quad (33)$$

The added mass matrix for infinite frequency $\mathbf{A}_\infty$ and the impulse response function $\mathbf{K}(t, \bar{\mathbf{V}}_\mathbf{u})$ can be obtained from hydrodynamic coefficients computed in the frequency domain without forward speed (added mass $\mathbf{A}(\omega)$ and radiation damping $\mathbf{B}(\omega)$) using:

$$\mathbf{A}_\infty = \lim_{w \to +\infty} \mathbf{A}(\omega) \quad (34)$$

$$\mathbf{K}(t, \bar{\mathbf{V}}_\mathbf{u}) = \frac{2}{\pi} \int_0^{+\infty} \mathbf{B}(\omega) \cos(\omega t) d\omega - \frac{2}{\pi} \left[\int_0^{+\infty} (\mathbf{A}(\omega) - \mathbf{A}_\infty) \cos(\omega t) d\omega \right] \mathbf{L_S}(\bar{\mathbf{V}}_\mathbf{u}) \quad (35)$$

The incident waves being modelled by superposition of N elementary Airy waves, the diffraction force can be written:

$$\tau_{dif,G}(t) = \Im \left(\sum_{i=1}^{N} \mathbf{F_{dif}}(\omega_{e,i}, \psi - \gamma_i) A_i e^{i(k_i(x \cos\gamma_i + y \sin\gamma_i) - \omega_i t)} \right) \quad (36)$$

Where :

- $\mathbf{F_{dif}}(\omega_{e,i}, \psi - \gamma_i)$ is the diffraction force coefficient in frequency domain for an incident wave of unit amplitude propagating in direction $\psi - \gamma_i$ and with frequency $\omega_{e,i}$
- A_i, k_i, ω_i are respectively the incident wave amplitude (complex number including phase), the wave number and the frequency of the component i of the incident wave.

The encounter frequency $\omega_{e,i}$ and the incident wave frequency ω_i are related by $\omega_{e,i} = \omega_i - k_i(\bar{u}\cos\gamma_i + \bar{v}\sin\gamma_i)$.

In this study, the frequency domain hydrodynamic coefficients $\mathbf{A}(\omega), \mathbf{B}(\omega)$ and $\mathbf{F_{dif}}(\omega, \gamma)$ were computed using the open-source software Nemoh Babarit and Delhommeau, 2015.

3.2 Oblique Towing Test

This section shows a first example of application of the method. The configuration is that of an oblique towing test with the 1/110 scale model. The propeller rotation velocity is 0. There are neither wind nor waves. The forced motion is such that:

$$\begin{cases} x(t) = Ut \text{ with } U = 0.763\,\mathrm{m\,s^{-1}} \text{ (corresponding to } 15\,\mathrm{kn} \text{ at full scale)} \\ y(t) = 0 \\ \varphi(t) = 0 \\ \psi(t) = 15° \end{cases} \tag{37}$$

The ship is free to move only in heave and pitch, thus the operator $T_{\Xi\lambda}$ reads:

$$T_{\Xi\lambda} = \begin{bmatrix} 0 & 0 \\ 0 & 0 \\ 1 & 0 \\ 0 & 0 \\ 0 & 1 \\ 0 & 0 \end{bmatrix} \tag{38}$$

For the operator $T_{\tau\mu}$, as noted previously, many options are possible provided that the elements of the third row (component of the extra force in the vertical direction) and sixth row (moment along the vertical axis of the extra force) are equal to zero. In this study, we chose the simplest possibility:

$$T_{\tau\mu} = \begin{bmatrix} 1 & 0 & 0 & 0 \\ 0 & 1 & 0 & 0 \\ 0 & 0 & 0 & 0 \\ 0 & 0 & 1 & 0 \\ 0 & 0 & 0 & 1 \\ 0 & 0 & 0 & 0 \end{bmatrix} \tag{39}$$

Figure 3 shows the simulated motion of the ship. One can see that it follows well the prescribed motion for those degrees of freedom which are forced, while the free motions exhibit damped oscillations as expected. Figure 4 shows the six components of the extra force. The z-component of the force and y-component of the moment are equal to 0 as expected. The other components tend to constant values after a few initial oscillations that can be attributed to radiation effects.

3.3 Forced heading

In this second example, the full-scale ship going forward in waves and wind is considered. The wind profile is uniform. The wind speed is $10\,\mathrm{m\,s^{-1}}$ and the true wind direction is $90°$ (wind blowing to the East). The incident wave is a regular wave of period $8\,\mathrm{s}$, wave height $2\,\mathrm{m}$ and wave direction $120°$. The propeller rotational speed is $99\,\mathrm{rpm}$.

Three configurations were simulated. In the first one, the 6 Degrees of Freedoms of the ship are enabled. No heading control system is specified. In Figure 5, one can see that the unbalance in the yaw-moment causes the ship to slowly deviates from its original $0°$ heading angle. At t = $300\,\mathrm{s}$, the heading is $-5°$. Furthermore, this phenomenon does not seem to dissipate with time. Longer simulations have been carried out. They show that the heading angle keeps decreasing with increasing simulation time ($-68°$ at t = $1200\,\mathrm{s}$).

In the second configuration, the ship heading is forced to $0°$. The operator $T_{\tau\mu}$, was set to the simplest

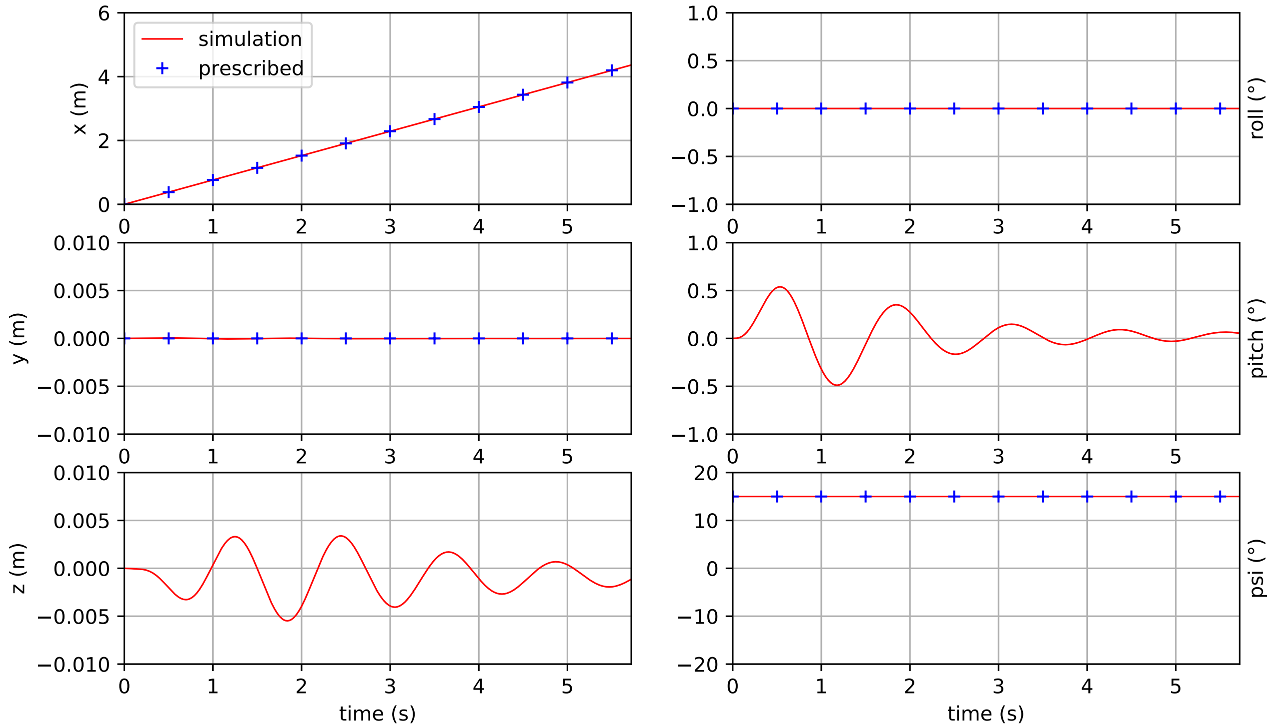

Figure 3. Motion of the ship in oblique towing test example

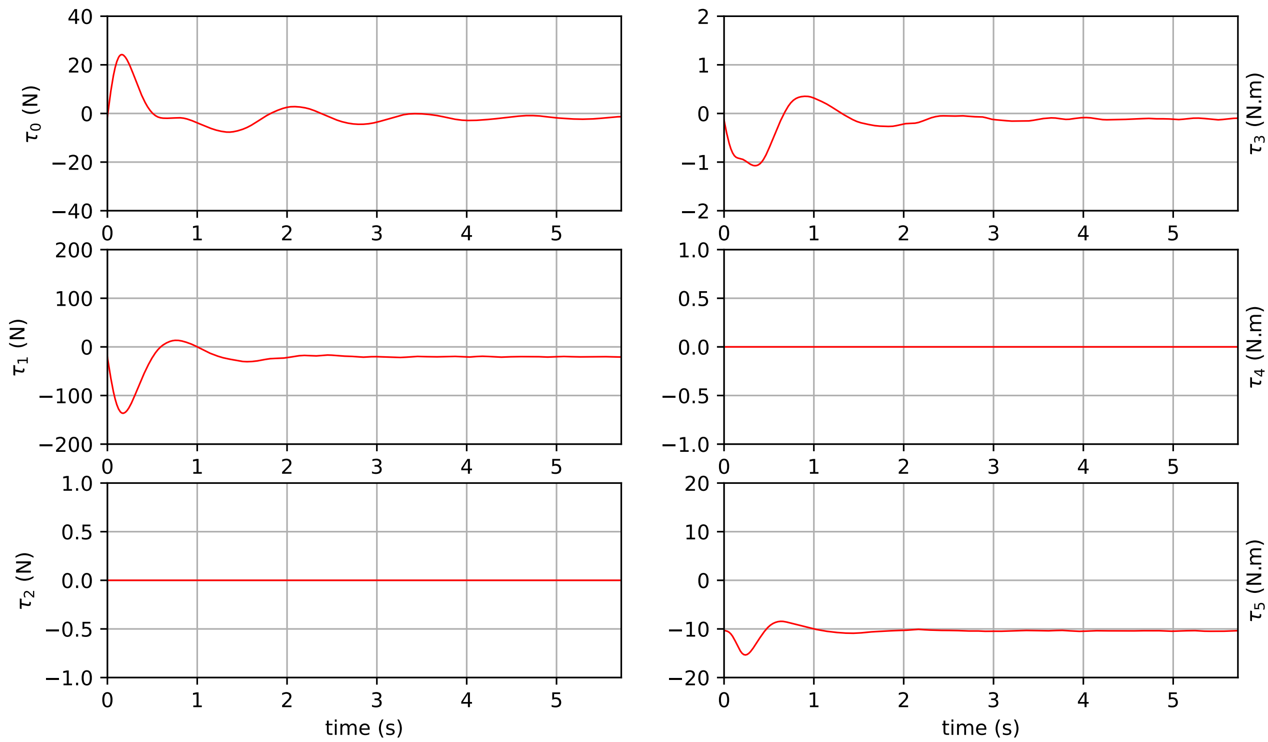

Figure 4. Extra force in oblique towing test example

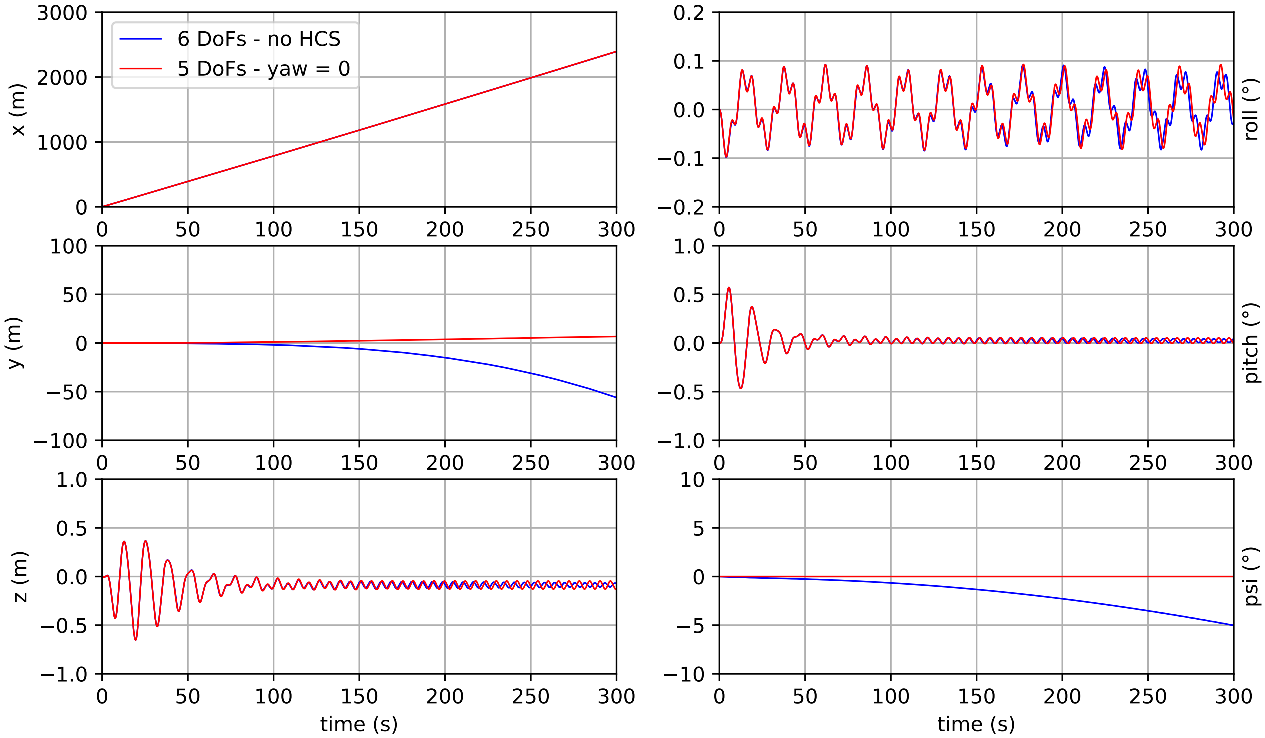

Figure 5. Motion of the ship without heading control and with heading forced to $0°$. Wave period is $8\,\mathrm{s}$, wave height is $2\,\mathrm{m}$, and wave direction is $120°$. True wind speed is $10\,\mathrm{m\,s^{-1}}$, wind direction is $90°$.

possibility $T_{\tau\mu} = \begin{bmatrix} 0 & 0 & 0 & 0 & 0 & 1 \end{bmatrix}^T$. Conversely, the operator $T_{\Xi\lambda}$ is

$$T_{\Xi\lambda} = \begin{bmatrix} 1 & 0 & 0 & 0 & 0 \\ 0 & 1 & 0 & 0 & 0 \\ 0 & 0 & 1 & 0 & 0 \\ 0 & 0 & 0 & 1 & 0 \\ 0 & 0 & 0 & 0 & 1 \\ 0 & 0 & 0 & 0 & 0 \end{bmatrix} \tag{40}$$

Figure 5 shows that, as expected, the ship heading remains constant (equal to $0°$) all over the simulation. Moreover, it can be observed that during the first hundred seconds of the simulation, the motions of the ship centre and both the roll motion and pitch motion of the ship are very similar to that of the simulation with 6 DoFs. Differences only start to be visible by the second half of the simulation. They can be attributed to the significantly different heading angles between the two configurations at that point in the simulation. All in all, this indicates that the proposed forcing motion method can be used as a simple heading control system with little to no effects on the ship response in the other degrees of freedom.

From the results shown in Figure 5, one can get the impression that, without heading control, the ship drifts towards $y < 0$, which would be surprising since the wind direction and the wave propagation direction are oriented towards $y > 0$. This effect actually results from the lack of heading control. Indeed, as can be seen in the Figure, the ship slowly rotates towards the wind due to unbalance of the moment in yaw (yaw motion is ψ = -5^o at the end of the simulation). Therefore, as the ship is moving forward and as the ship bow points more and more towards $y < 0$, the ship trajectory gets deviated towards $y < 0$.

In the previous configuration, forced heading is achieved by applying a pure yaw moment (only the sixth component of the operator $T_{\tau\mu}$ is different from 0). In practice, heading control is achieved thanks

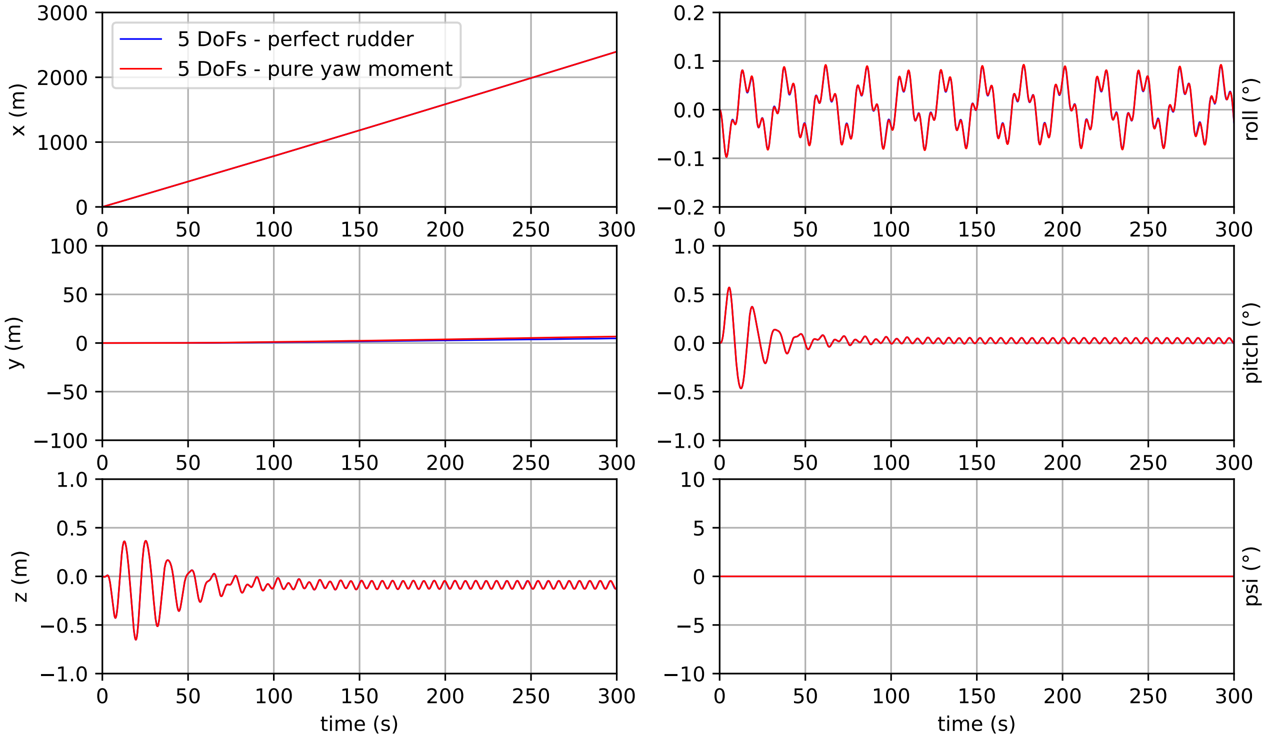

Figure 6. Comparison of the motion of the ship with forced heading angle with a pure yaw moment for the extra force and with an extra force model mimicking the effect of a perfect rudder.

to the rudder action. A pure yaw moment is poorly representative of the physical effect of the rudder. Indeed, a rudder essentially generates a side force. It is the fact that this side force is generated far from the ship centre that leads to a yaw moment which can be significant. Therefore, a more representative model of the ship with perfect heading control system can be obtained by using the operator $T_{\tau\mu} = \begin{bmatrix} 0 & 1 & 0 & 0 & 0 & \chi_{rd} \end{bmatrix}^T$ with χ_{rd} be the x-coordinate of the rudder axis in the ship-fixed reference frame.

Figure 6 shows a comparison of the motion response of the ship with forced heading achieved by applying a pure yaw moment (configuration 2 labelled pure yaw moment in the figure) and by applying a pure side force at the rudder axis (configuration 3 labelled perfect rudder in the figure). Figure 6 shows a comparison of the extra force in the two configurations. $\chi_{rd} = -170\,\mathrm{m}$ in the case study. One can see despite the differences in the extra force models ($T_{\tau\mu}$ operator), the differences in the motion response are hardly visible. This is due to the side force component of the extra force being small in comparison to other forces. Overall, it seems that using a pure yaw moment for the extra force required to achieve a fixed heading is quite acceptable.

4 CONCLUSION

In this study, a method to force a number of degrees of freedom in ship simulators has been proposed. It is based on the forcing of the second derivatives of the forced degrees of freedom. The method has been implemented in the open-source simulator *xdyn*. Examples of simulations of oblique towing tests and forced heading have been presented which show that the method works as expected.

The authors believe that the proposed method is beneficial for the ocean engineering community because it allows both the modelling of a ship using modern formulations of its equation of motion and the forcing of some of its degrees of freedom. An example is that is allows the forcing of the ship heading without the difficult task of having to specify a heading control system. Furthermore, the forcing force can be used by the naval architect for the design of the heading control system and

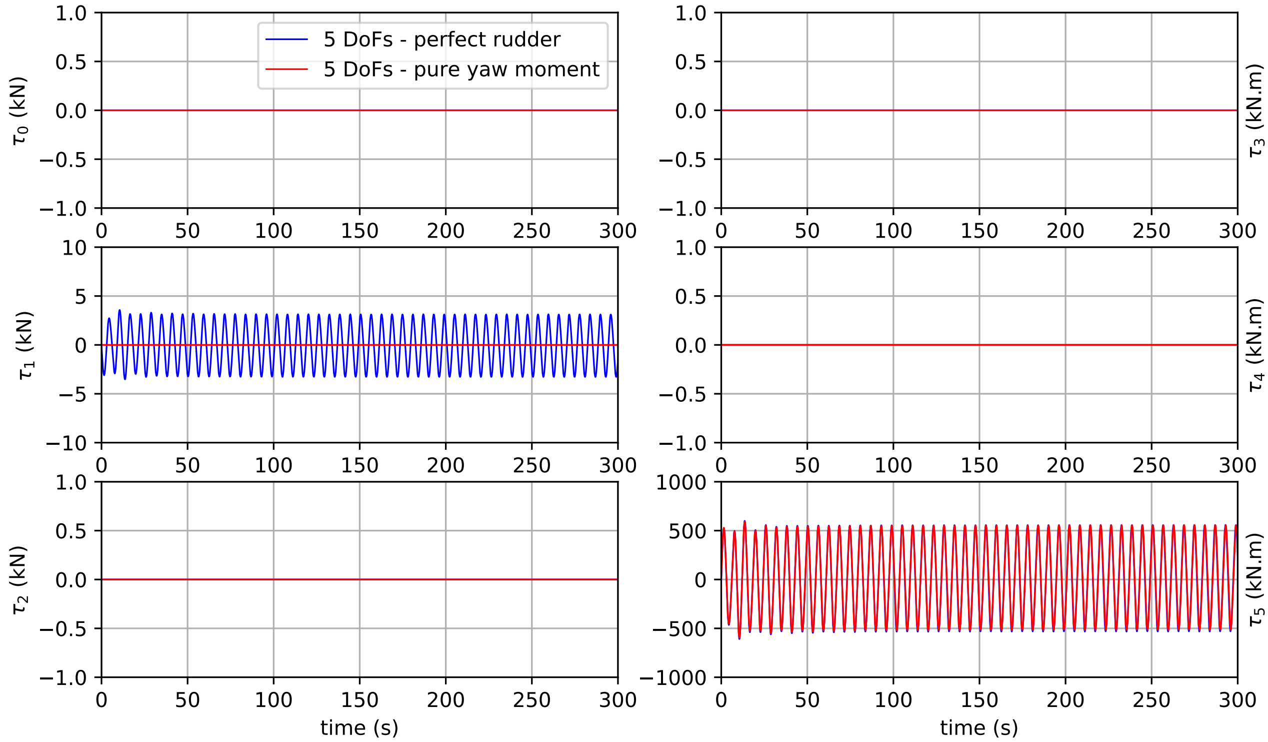

Figure 7. Comparison of the extra force for the ship with forced heading angle with a pure yaw moment for the extra force and with an extra force model mimicking the effect of a perfect rudder.

appendages.

The method requires an explicit relationship between the second derivatives of the degree of freedom and the acceleration vector. Such relationship is provided in this paper for the Cardan/Tait-Bryan angles convention. Similar relationships for other angles convention remain to be derived, which has been left for future work. Moreover, future work may consider coupling the proposed method to the articulated-body algorithm to deal with, for example, ships equipped with cranes.

APPENDIX

The rotation matrix $\mathbf{R}_{\text{NED},b}$ can be written as function of the quaternion components as:

$$\mathbf{R}_{\text{NED},b} = \begin{bmatrix} q_r^2 + q_i^2 - q_j^2 - q_k^2 & 2(q_i q_j - q_r q_k) & 2(q_i q_k + q_r q_j) \\ 2(q_i q_j - q_r q_k) & q_r^2 + q_i^2 - q_j^2 - q_k^2 & 2(q_j q_k - q_r q_i) \\ 2(q_i q_k + q_r q_j) & 2(q_j q_k - q_r q_i) & q_r^2 + q_i^2 - q_j^2 - q_k^2 \end{bmatrix} \tag{41}$$

Its derivative is:

$$\dot{\mathbf{R}}_{\text{NED},b} = 2 \begin{bmatrix} q_r\dot{q}_r + q_i\dot{q}_i - q_j\dot{q}_j - q_k\dot{q}_k & \dot{q}_i q_j + q_i\dot{q}_j - \dot{q}_r q_k - q_r\dot{q}_k & \dot{q}_i q_k + q_i\dot{q}_k + \dot{q}_r q_j + q_r\dot{q}_j \\ \dot{q}_i q_j + q_i\dot{q}_j - \dot{q}_r q_k - q_r\dot{q}_k) & q_r\dot{q}_r + q_i\dot{q}_i - q_j\dot{q}_j - q_k\dot{q}_k & \dot{q}_j q_k + q_j\dot{q}_k - \dot{q}_r q_i - q_r\dot{q}_i \\ \dot{q}_i q_k + q_i\dot{q}_k + \dot{q}_r q_j + q_r\dot{q}_j & \dot{q}_j q_k + q_j\dot{q}_k - \dot{q}_r q_i - q_r\dot{q}_i & q_r\dot{q}_r + q_i\dot{q}_i - q_j\dot{q}_j - q_k\dot{q}_k \end{bmatrix} \tag{42}$$

ACKNOWLEDGEMENTS

This work was partially funded by the Carnot Institute ”Marine Engineering Research for Sustainable, Safe and Smart Seas”.

REFERENCES

(ORC), Offshore Racing Congress (2021). *ORC VPP Documentation 2021*. Tech. rep.

Babarit, A. and Delhommeau, G. (2015). Theoretical and numerical aspects of the open source BEM solver NEMOH. *11th European Wave and Tidal Energy Conference* (Nantes, France).

Bernitsas, M.M., Ray, D., and Kinley, P. (1981). *KT, KQ and efficiency curves for the Wageningen B-series propellers*. Tech. rep. The university of Michigan.

Blendermann, W. et al. (1993). *Maneuvoeuvring Technical Manual*. Seehafen Verlag.

Bougis, J. (1980). Etude de la diffraction-radiation dans le cas d'un flotteur indéformable animé d'une vitesse moyenne constante et sollicité par une houle sinusoidale de faible amplitude. PhD thesis. Ecole Nationale Supérieure de Mécanique.

Cairoli, C. (2000). Analysis of the IMS velocity prediction program. MA thesis. University of Virginia.

Cha, J-H., Roh, M-I., and Lee, K-Y. (2010). Dynamic response simulation of a heavy cargo suspended by a floating crane based on multibody system dynamics. *Ocean engineering* 37 (14-15), pp. 1273–1291.

Charlou, M. (2023). Méthodes et outils d'aide à la conception pour l'assistance à la propulsion éolienne des navires. PhD thesis. Ecole Centrale Nantes.

Charlou, M., Babarit, A., and Gentaz, L. (2022). A new validated open-source numerical tool for the evaluation of the performance of wind-assisted ship propulsion systems. *Proc. of the 25^{e} Congrès Francais de Mécanique* (Nantes, France).

Charlou, M., Babarit, A., and Gentaz, L. (2023). A new validated open-source numerical tool for the evaluation of the performance of wind-assisted ship propulsion systems. *Mechanics & Industry* 24.26.

Day, S., Letizia, L., and Stuart, A. (2002). VPP vs PPP: challenges in the time-domain prediction of sailing yacht performance. *High performance yacht design conference* (Auckland, New zealand).

Featherstone, R. (2008). *Rigid body dynamics algorithms*. Springer.

Fossen, Thor I. (2011). *Handbook of Marine Craft Hydrodynamics and Motion Control*. John Wiley Sons.

Gerritsma, J., Keuning, J.A., and Versluis, A. (1993). Sailing Yacht Performance in Calm Water and Waves. *Proc. of the 11th Chesapeake sailing yacht symposium* (Annapolis, MD, USA), pp. 233–246.

Ham, S-H. et al. (2015). Multibody dynamic analysis of a heavy load suspended by a floating crane with constraint-based wire rope. *Ocean engineering* 109, pp. 145–160.

Harris, D.H. (2005). Time domain simulation of a yacht sailing upwind in waves. *The 17th Chesapeake sailing yacht symposium* (Annapolis, MD, USA).

Henderson, D. M. (1977). *Shuttle program. Euler Angles, quaternions, and transformation matrices. Working relationships*. Tech. rep. NASA.

Holtrop, J. and Mennen, G.G.J. (1982). An Approximate Power Prediction Method. *International Shipbuilding Progress* 29.335, pp. 166–170.

Horel, B. (2016). Modélisation Physique du Comportement du Navire par Mer de l'Arrière. PhD thesis. Ecole Centrale de Nantes.

Kerdraon, P., Leplingard, A., and Guisnel, X. (2023). Comprehensive design flow for appendage modal analysis and flutter investigation. *Proc. of the 6th International Conference on Innovation in High Performance Sailing Yachts and Wind-Assisted Ships* (Lorient, France), pp. 159–171.

Kerdraon, P. et al. (2020). Development of a 6-DOF Dynamic Velocity Prediction Program for offshore racing yachts. *Ocean engineering* 212.107668.

Kim, Y. et al. (2011). Time-domain analysis of nonlinear motion responses and structural loads on ships and offshore structures: development of WISH programs. *Inter. J. Nav. Archit. Oc. Engng* 3, pp. 37–52.

Kjellberg, M., Gerhardt, F., and Werner, S. (2023). Sailing Performance of Wind-Powered Cargo Vessel in Unsteady Conditions. *Proc. of the 6th International Conference on Innovation in High Performance Sailing Yachts and Wind-Assisted Ships* (Lorient, France), pp. 281–306.

Kostia, R. and Kobus, J.M. (2004). Dynamic simulation of two sailing boats in match racing. *Sports engineering* 7, pp. 139–152.

Kring, D. et al. (1996). Nonlinear ship motions and wave-induced loads by a Rankine panel method. *Proc. of the 21st symposium on naval hydrodynamics* (Trondheim, Norway), pp. 45–63.

Negrut, D. (1998). On the implicit integration of differential-algebraic equations of multibody dynamics. PhD thesis. University of Iowa.

Oliver, J.C., Letcher Jr, J.s., and Salvesen, M. (1987). Performance predictions for stars & stripes. *SNAME Trans.* 95, pp. 239–261.

Poor, C.L. (1986). *A description of the new international rating system*. Tech. rep. Publication of the United States Yacht racing union.

SIMMAN 2008 : Workshop Verification and Validation of Ship Manoeuvring Simulation Methods (n.d.). `http://www.simman2008.dk/KVLCC/KVLCC2/tanker2.html`. Accessed: 2023-06-12.

Tillig, F. and Ringsberg, J.W. (2020). Design, operation and analysis of wind-assisted cargo ships. *Ocean engineering* 211.107603.

Wuillaume, P-Y. et al. (2021). Numerical simulation of lowering operations from the coupling between the Composite-Rigid-Body Algorithm and the weak-scatterer approach. *Ocean engineering* 241.109997.

xdyn (n.d.). `https://gitlab.com/sirehna_naval_group/sirehna/xdyn`. Accessed: 2023-06-12.

Yasukama, H. and Yoshimura, Y. (2015). Introduction of the MMG standard method for ship maneuvering predictions. *J. Mar. Sci. Technol.* 20, pp. 37–57.